



Physical Properties of Sputtered CdTe Thin Films

KEYWORDS

CdTe films, sputtering, semiconductor

E. Camacho-Espinosa

Centro de Investigación en Dispositivos Semiconductores, BUAP, 14 Sur y Avenida San Claudio, C. U. Edificio 103-C, C.P. 72570 Puebla, Puebla México.

E. Rosendo

Centro de Investigación en Dispositivos Semiconductores, BUAP, 14 Sur y Avenida San Claudio, C. U. Edificio 103-C, C.P. 72570 Puebla, Puebla México.

A.I. Oliva

Centro de Investigación y de Estudios Avanzados del IPN Unidad Mérida. Depto. Física Aplicada. Km. 6 Antigua Carretera a Progreso, A.P. 73-Cordemex C.P. 97310 Mérida Yucatán México.

T. Díaz

Centro de Investigación en Dispositivos Semiconductores, BUAP, 14 Sur y Avenida San Claudio, C. U. Edificio 103-C, C.P. 72570 Puebla, Puebla México.

N. Carlos-Ramírez

Centro de Investigación en Dispositivos Semiconductores, BUAP, 14 Sur y Avenida San Claudio, C. U. Edificio 103-C, C.P. 72570 Puebla, Puebla México.

H. Juárez

Centro de Investigación en Dispositivos Semiconductores, BUAP, 14 Sur y Avenida San Claudio, C. U. Edificio 103-C, C.P. 72570 Puebla, Puebla México.

G. García

Centro de Investigación en Dispositivos Semiconductores, BUAP, 14 Sur y Avenida San Claudio, C. U. Edificio 103-C, C.P. 72570 Puebla, Puebla México.

M. Pacio

Centro de Investigación en Dispositivos Semiconductores, BUAP, 14 Sur y Avenida San Claudio, C. U. Edificio 103-C, C.P. 72570 Puebla, Puebla México.

ABSTRACT In this work, CdTe thin films were deposited on glass substrates by sputtering technique at different pressures and rf-power conditions. Morphology, growing parameters, and the crystalline structure were studied as a function of the work pressure (2 to 40 mTorr) and the rf-power (25 to 45 W). The deposition rate increases from 1.5 to 6.0 nm/min when the work pressure decreases. In a similar way, the deposition rate changes from 2.5 to 6.0 nm/min when the rf-power ranges from 25 to 45 W. The optical bandgap energy values of the deposited CdTe films ranged from 1.36 to 1.6 eV. The surface roughness of the films was found to be independent on the work pressure and the rf-power conditions. The crystalline structure of the deposited films improves for lower work pressures and higher rf-powers. Better conditions for films deposition were found at 5 mTorr and 35 W.

1. INTRODUCTION

Despite all the research carried out on the semiconducting CdTe films, scarce work has been reported on the characterization of such films deposited by the sputtering technique, commonly used for low-cost solar cells manufacturing. In the last three decades, several studies on the CdTe films preparation have been reported such as diluted magnetic semiconductor, nonlinear optics, and photovoltaic devices [1-3]. Among the most cited applications on CdTe, the use of this film as an absorbent layer in a CdS/CdTe solar cell can be highlighted, due to its very high absorption coefficient $> 10^4 \text{ cm}^{-1}$ which allows absorbing 99% of the incident light in a 2 μm thick film [4, 5]. Semiconducting CdTe has a direct band gap energy ($E_g = 1.5 \text{ eV}$, at room temperature) near to the optimum value for efficient solar energy conversion [6]. Several physical and chemical techniques for CdTe films preparation have been reported such as closed space sublimation (CSS) [7], molecular beam epitaxy (MBE) [8], electrodeposition [9], pulsed laser deposition (PLD) [10, 11], metal organic chemical vapor deposition (MOCVD) [12], successive ionic layer adsorption and reaction method (SILAR) [13], and spray pyrolysis [14]. A commonly physical technique used for CdTe film deposition is magnetron rf-sputtering [6, 15]. This technique makes possible to obtain films with the same stoichiometry than that of the sputtered target, making it a suitable technique to fabricate intermetallic compounds [16]. The main advantage of the sputtering technique is the use of low energy particle bombardment for achieving lower growth temperatures along with the use of excited species for improving

the doping control during growth [17].

However, several issues have not been yet solved regarding the rf-sputtering technique, e.g. the control of the grain size for films deposited at room temperature. The importance of the grain size investigation lies in the relation with the number of recombination centers and potential barriers that affect the solar cell performance [18]. Desirable characteristics of the CdTe layer for solar cells applications are large crystals and flat surfaces [19].

In this work, the morphological, optical, and structural properties of CdTe films deposited by sputtering technique on glass substrates at different radio frequencies (rf) powers and work pressures were studied. Better experimental conditions for the CdTe films deposition were determined. This work contributes to improve the quality of sputtered-CdTe thin films to be used for different technological applications.

2. EXPERIMENTAL PROCEDURE

Thin films of CdTe were deposited by sputtering onto glass substrates ($70 \times 15 \times 1.1 \text{ mm}^3$) at room temperature. A commercial CdTe target of 99.999% purity and one inch-diameter was employed. The base pressure of the vacuum chamber was $1 \times 10^{-5} \text{ Torr}$, and substrates were separated 11 cm from the target during the film deposition. In order to study the optical and structural changes in the CdTe films in terms of the deposition parameters, two batches were prepared as follows. In the first batch, five samples were prepared at work

pressures from 2 to 40 mTorr; while the rf-power and deposition time were fixed at 40 W and 2 h, respectively. The work pressure was controlled by introducing argon gas. The range of pressures was determined based on early experimental observations. The lowest work pressure of 2 mTorr is near to the lowest pressure value required to keep the plasma (1 mTorr). On the other hand, no CdTe deposition occurs with a work pressure higher than 50 mTorr, due to the excessive amount of Ar ions, which dramatically reduces the mean free path of the atoms avoiding the deposition onto the substrate.

In the second batch, five samples were prepared from 25, to 45 W as rf-power, while the pressure and deposition time were fixed at 5 mTorr and 2 h, respectively. The rf-power range was chosen between the very low deposition rate observed below 25 W and the maximum power density recommended by the supplier (60 W/in²) for materials with low thermal conductivity, such as CdTe. Thus, for the target of 0.785 in²-area (1 inch- diameter) the maximum rf-power value to be applied was 45 W. Higher power value than 45 W increases the temperature and produces damages in the magnetron. The thickness of the deposited films was measured with a profilometer Dektak 150 where standard scans of 5 mm-length and tip force of 2.9 mN were carried out. The surface morphology of the deposited CdTe films was measured with an Ambios Universal AFM in non-contact mode. Optical transmittance/absorbance of the deposited films were measured with a double beam Cary 5000 UV-VIS-NIR spectrophotometer in the wavelength range of 300 to 2500 nm in order to estimate the bandgap energy (E_g) value. The crystalline structure was measured with a Bruker AXSD8 Discover diffractometer with a Cu_α ($\lambda=1.5405 \text{ \AA}$) beam. The measurements were recorded for a diffraction angle 2θ ranging from 20° to 80° in steps of 0.02°.

RESULTS AND DISCUSSION

2.1 Deposition rate and thickness

The thickness of the CdTe films fabricated with constant deposition time (2 h) was measured in order to determine the deposition rate. Figure 1 shows the thickness and the deposition rate of the films as a function of the work pressure for a rf-power of 40 W. From the obtained results, it can be observed that the deposition rate increases when the work-pressure decreases. This behavior can be explained in terms of the mean free path, which promotes that the sputtered atoms suffer minor collisions before reaching the substrate. In Figure 1, a rapid increase in the deposition rate can be observed from 10 mTorr to lower work pressure values resulting in deposition rates values from 3 to 6 nm/min. These values are in good agreement with the values reported by Wang et al. [20] which range from 2 to 4.5 nm/min, for work pressures between 7.5 and 68 mTorr for $\text{Zn}_x\text{Mg}_x\text{O}$ films.

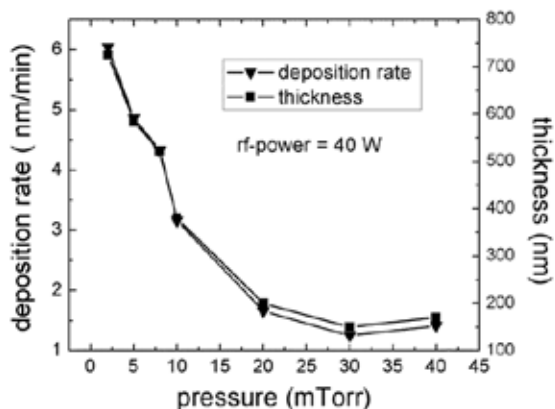


Figure 1. Film thickness and deposition rate of CdTe thin films as a function of the work pressure.

Figure 2 shows the deposition rate and the film thickness

as a function of the sputtering rf-power. An increase on the deposition rate can be observed in Fig. 2, as the rf-power increases. Given that the sputtering rate depends on the current of ions and on the sputtering performance (proportional to the energy), it is therefore suggested that the deposition rate is proportional to the applied power [21]. A minimum value of 2.5 nm/min as deposition rate was obtained for 25 W; meanwhile, a maximum value of 6 nm/min was obtained for 45 W. The deposition rate with rf-power does not present a linear behavior.

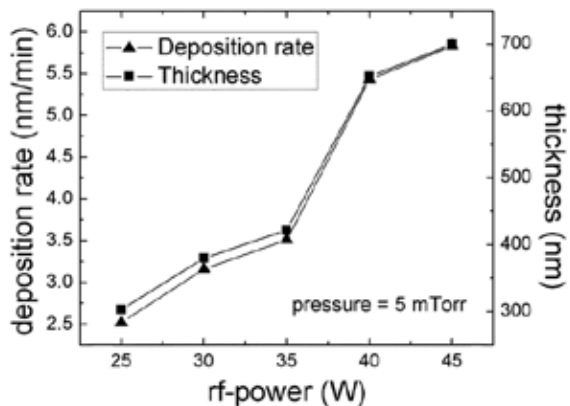


Figure 2. Film thickness and deposition rate of CdTe thin films as function of the rf-power.

2.2 Morphology

The AFM images show that the film surface is formed by small and rounded grains; typically observed for sputtered materials [22, 23]. Small imaging areas were obtained to better appreciate the grain size and their shapes.

According to the scaling law, during the growing process, an increase on the film thickness corresponds to an increase of the grain size [24] until saturation. This behavior can be observed in the AFM images in Figure 3, where a sequence of CdTe films deposited at different pressures is presented. As can be observed, the grain size, i.e., film thickness, increases with the work pressure reduction. This behavior can be understood in terms of the growth process which is described as follows: the atoms arrive to the substrate and are adsorbed. Adsorbed atoms move over the substrate interacting between them and forming clusters. As the clusters collide with the adsorbed species, they achieve certain critical size reaching a thermodynamic stability. Such a behavior occurs when the nucleation barrier is overcome. Finally, the number and size of the critical nucleus become higher, until a saturation nucleation density is reached rendering the layers formation. However, grain size is limited by two important factors: the energy of incident species and the surface mobility.

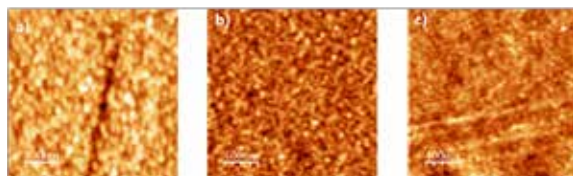


Figure 3. AFM images ($2 \times 2 \mu\text{m}^2$) from CdTe deposited at different work pressures: a) 2 mTorr, b) 8 mTorr, and c) 40 mTorr.

Due to the substrate temperature condition used at the CdTe deposition process (room temperature), the surface mobility results to be low, affecting the grain growth. On the other hand, an increase on the kinetic energy (rf-power) increases the surface mobility.

However, at even higher energies, the surface mobility is reduced due to the penetration of incident species into the

substrate, resulting in a smaller grain size.

Figure 4 shows the AFM images of the CdTe films deposited at different rf-powers. It is observed that the grain size increases with the increase of power, being the later related to the film thickness increase as previously discussed. Grain sizes can be explained as a consequence of the growth process as explained for the films growth at different work pressure.

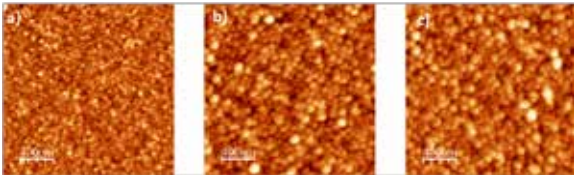


Figure 4. AFM images ($2 \times 2 \mu\text{m}^2$) from CdTe deposited at different rf-powers: a) 25 W, b) 35 W, and c) 45 W.

The roughness value of the films surface was determined from the obtained AFM images. Because of the irregular surface roughness along the sample, homogeneous areas were chosen on each film for the roughness measurement. The mean value of the rms-roughness obtained for the CdTe films deposited with different pressures was 0.85 nm, meanwhile for films with different rf-powers was 0.64 nm, a slightly lower value. Thus, the pressure and the rf-power values do not have significant influence on the rms-roughness of the deposited CdTe films. However, most of the obtained roughness values are about the half of the values reported for different materials deposited by sputtering, which range from 1.0 to 1.8 nm [25, 22]. Figure 5 presents the rms-roughness of the sputtered films as a function of the vacuum pressure and the rf-power. A continuous increase in roughness is observed with the increase of rf-power which corresponds to thicker films; meanwhile a maximum roughness value is observed for films deposited at 20 mTorr. This behavior is in good agreement with the results reported by Yan and Woolam [25] where they studied the roughness of dc magnetron sputtered iridium films. In their work, authors report a proportional increment of roughness with thickness. Thus, during the growth of the films the roughness increases until a saturation limit is reached.

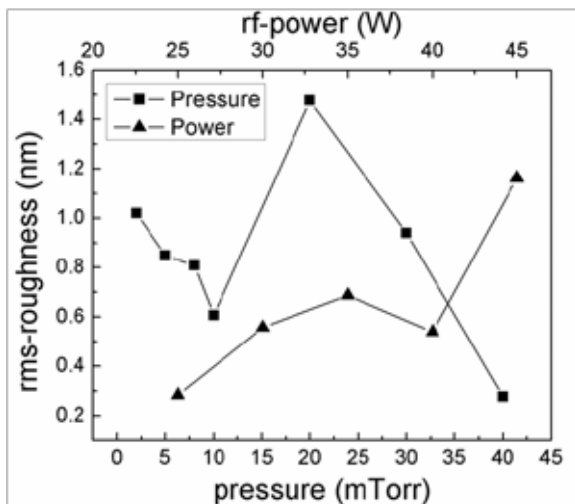


Figure 5. Rms-roughness as a function of the work pressure and the rf-power.

2.3 Crystalline structure

X-ray diffractograms of the CdTe films deposited at different pressures were obtained and their corresponding results are shown in Figure 6. From the diffraction patterns of the CdTe films, the observed peaks correspond to the (111), (220) and (311) orientations at the 2θ values of 23.7° , 39.2° , and 46.4° , respectively. Such an observed XRD pattern for the CdTe

films corresponds to a cubic centered face structure (FCC).

From Fig. 6, it can be observed that the peak intensities increase as the work pressure decreases, which indicates more order in the crystalline structure for the CdTe films deposited at lower work pressure. The improved crystalline structure of the films at lower work pressure may be caused by the increase on the diffusivity of the deposited atoms on the substrate, promoting the film growth in the (111) orientation as compared with the lower surface energy for the (220) and (311) orientations [26].

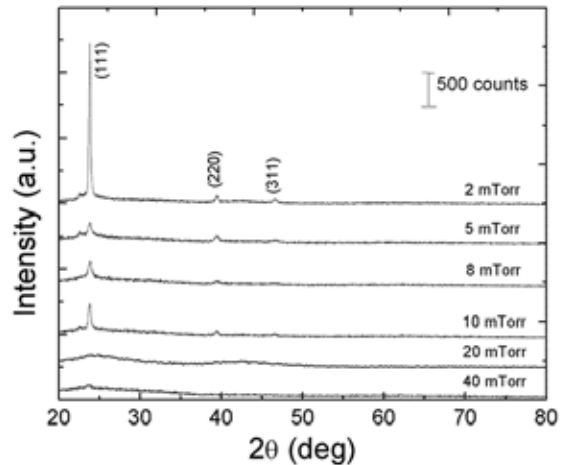


Figure 6. XRD patterns of CdTe films deposited at different work pressures.

By determining the full-width at half-maximum (FWHM) parameter from the (111) orientation, the crystallite size D of the films can be calculated by the Debye-Scherrer formula given by [27],

$$D = 0.9\lambda/\beta \cos \theta \quad (1)$$

where λ is the wavelength ($\lambda = 1.5408 \text{ \AA}$) of the x-ray radiation, β is the FWHM of the peak, and θ is the Bragg's angle. The lattice parameter was also calculated in order to investigate its change after a possible recrystallization process.

Changes in the lattice parameter are usually associated to strains in the films, which are present in films deposited at lower substrate temperatures [28]. On the other hand, strains can also be related to a net driving force which is composed by two parts: the first one is the stored energy of deformation and the second is the grain boundary energy [29]. The mentioned driving forces are caused by dislocations, excess of free energy in the interfaces and plastic deformations.

Figure 7 shows the estimated crystallite size and lattice parameter vs work pressure of the cubic CdTe films. From Fig. 7, an increase of the crystallite size at higher pressures can be observed. The experimental trends observed in Fig. 7 can be qualitative explained by means of the following expression [30],

$$\lambda = 2.33 \times 10^{-20} (T/P \delta_m^2) \quad (2)$$

where λ (cm) is the mean free path, T is the absolute temperature, P is the pressure in Pa, and δ_m (cm) is the molecular diameter. As observed in Eq. 2, the pressure is inversely proportional to the mean free path; this indicates that for high pressure, mean free path is small i.e. atoms collide at short distances. It can be therefore suggested that at high pressures, the sputtered atoms undergo a large number of collisions which significantly increases the probability of agglomeration i.e., an increment in the crystallite size before arriving at the surface of the substrate.

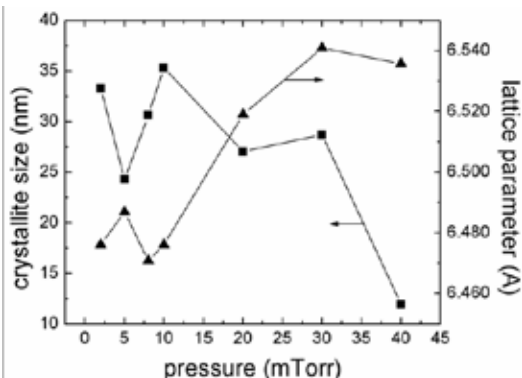


Figure 7. Crystallite size and lattice parameters obtained from the XRD patterns as a function of the work pressure.

Experimentally, a change in the 2θ position of an x-ray diffraction peak, gives a change in the lattice parameter. In order to estimate these changes, the lattice parameter a can be calculated by considering the cubic (111) orientation of the CdTe films in Fig. 6, by the relation,

$$a = \sqrt{3} n\lambda / 2 \sin \theta \quad (3)$$

where n is the diffraction order. Analyzing equation 3, as the θ value increases, the lattice parameter a decreases producing compressive stress [31]. So that shifts to the right of the diffraction peaks means a compressive and shifts to the left will indicate tensile stress.

It is known that defects like vacancies present different effects on the lattice parameter value. Another cause of changes in the lattice parameter is the random distribution of grain sizes from one region to another, promoting microstrains. Moreover, if the crystals present complex shapes and random orientations, they also can induce microstrains [31]. Thus, changes in the lattice parameter are mainly attributed to vacancies, because shape and size seems uniform.

Figure 7 shows a lattice parameter vs work pressure plot, where the lattice parameter value calculated for films deposited from 2 to 10 mTorr, is minor than the un-stressed value (a=6.4810 Å) [32]. However, the lattice parameter (a=6.535 Å) value for CdTe films deposited at 40 mTorr present higher values than the un-stressed value.

From Figure 8, we observe that intensity of the diffraction peak corresponding to the (111) orientation increases as rf-power increases, being this behavior related to a better crystallinity on the sample. Chan and Teo [33] attributed this effect to an improved electron mobility promoted by the increase of the kinetic energy of the adatoms sputtered on surface, which is required for obtaining films with high crystalline structure.

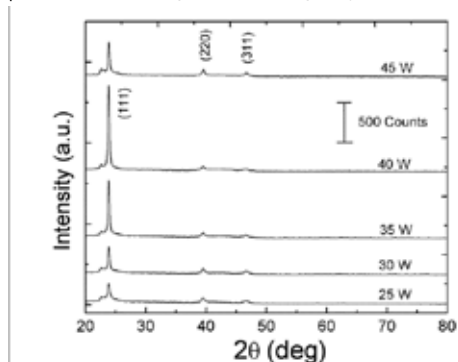


Figure 8. XRD patterns of CdTe films deposited at different rf-powers.

Figure 9 shows the behavior of the crystallite size and lattice parameter in terms of the rf-power. From Figure 9 a like-bellshape behavior is observed. The crystallite size increased from 21.2 to 23.5 nm when the rf-power increases from 25 to 35 W indicating an improvement in the crystalline structure; and a reduction at 21.7 nm for 45 W. A similar behavior was published by Reddy et al. [34] for nanocrystalline ZnO films. The maximum value of crystallite size at 35 W is associated with the change of the kinetic energy of the sputtered particles with their power [35]. Our obtained crystallite size values show good agreement with the values reported by Huimin et al. [26].

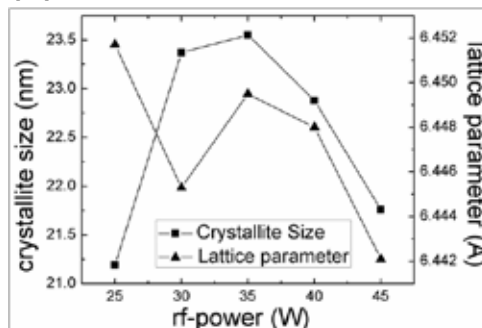


Figure 9. Crystallite size and lattice parameter values as a function of the rf-power.

Additionally, from figure 9, the lattice parameter decreases from 6.452 to 6.442 Å with the increment of the rf-power. A similar tendency was reported by Kumar et al. [36] for zinc aluminum oxide deposited by sputtering, where they reported more stressed films for the high sputtering power, attributing this behavior by the collision process during growth.

2.4 Bandgap energy

The direct optical bandgap (E_g) of the CdTe films deposited at different work pressures and rf-powers were calculated from the optical absorption results. The E_g values were estimated from the (αhv)² vs photon energy (hv) plots by a linear extrapolation on each absorption edge in the absorbance curve with α = 0 in the energy axis [37].

The measured E_g values for CdTe films deposited at different work pressures ranged between 1.44 and 1.60 eV and are shown in Figure 10. These values are very close to the E_g value reported for the bulk, E_g=1.52 eV, at 300 K [38]. Our E_g results are in good agreement with the values reported by other authors. For example, Ikhmayies et al., [5] reported a E_g=1.48 eV value for vacuum evaporated CdTe films prepared with substrates at room temperature. Choi et al. [15], estimated the bandgap energy from 1.41 to 1.45 eV for sputtered CdTe films with constant thickness but deposited under different pressure conditions from 1 to 80 mTorr. Pandey et al. [11] reported values of E_g=1.6 eV value for cubic CdTe films and E_g=1.54 eV for hexagonal CdTe films deposited by pulsed laser ablation.

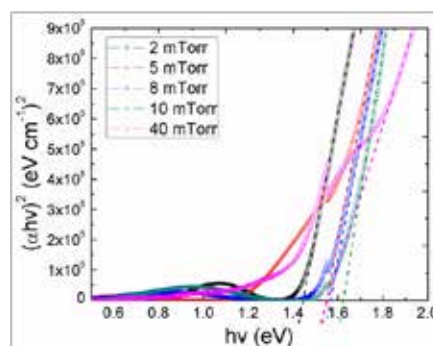


Figure 10. Tauc plots of (αhv)² vs energy (hv) for the CdTe films deposited at different work pressures.

For the CdTe films deposited with different rf-powers, the estimated E_g values ranged between 1.36 and 1.5 eV, and presented minor dispersion than the observed on the films deposited at different work pressures. The results of the bandgap energy are described in Figure 11. Our reported E_g values seems very similar to the values reported by Khan et al. [39] from 1.47 to 1.5 eV for vacuum evaporated CdTe films deposited on different substrates.

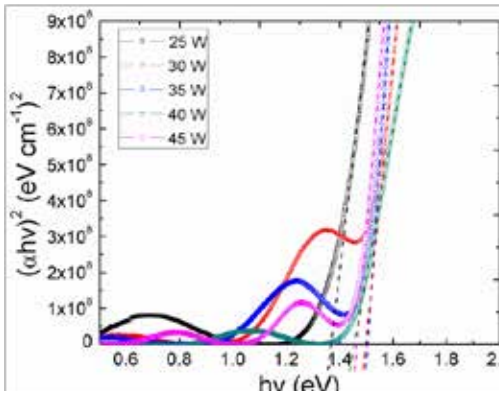


Figure 11. Tauc plot of $(Ahv)^2$ vs energy (hv) for the CdTe thin films deposited at different rf-powers.

Finally, Figure 12 shows the behavior of the E_g values of the CdTe films deposited at different work pressures and rf-powers. The horizontal line shows the CdTe bulk value as a reference.

From Figure 12, the E_g values for the CdTe films deposited with different rf-powers are lower than the bulk value (1.52 eV). These reduced values are associated with the tails in the edge of the bands which are produced by the disorder and imperfections in the lattice [5]. Therefore, from Figure 12 is inferred that work pressure presents a direct relation with the narrowing of the bandgap energy, given that all films deposited at different rf-powers and low work pressure (2 and 5 mTorr) presented E_g values below the bulk. On the other hand, films deposited at work pressures higher than 5 mTorr presented bandgap energy values above the reported for the bulk.

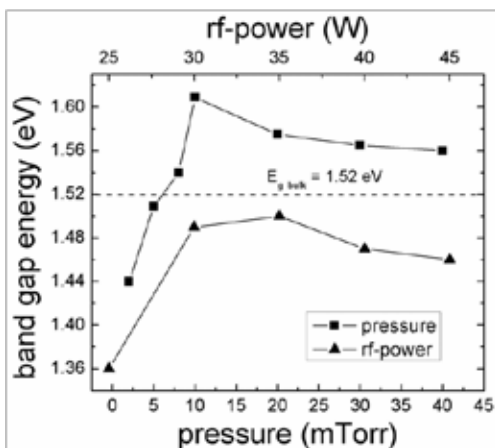


Figure 12. Bandgap energy values of the CdTe thin films deposited at different work pressures and rf-powers.

The work of Musil [40] explains that minor grain size, increases the grain boundaries so that CdTe film behaves different than bulk. Thus, we can affirm that the effects of the grain boundaries prevail over the bulk. The reduced grain size in the CdTe films with the increase of the work pressure can be observed in Figure 3.

3. CONCLUSIONS

The influence of rf-power and work pressure conditions on the morphology, growing parameters and crystalline structure of sputtered-CdTe thin films were investigated. The CdTe crystallinity was observed to increase with the increase of rf-power, having a maximum value at 35 W, and to decrease with the increase of the work pressure with a higher value at 10 mTorr. The film roughness was found to be independent of the rf-power and the work pressure, whereas a strong dependence with the film thickness was observed. The crystalline structure of deposited films improves for minor work pressures and with the increase of the rf-power. For films deposited with the maximum rf-power, the crystallinity is reduced by the re-sputtering effect.

Values of the bandgap energy below the bulk value (1.52 eV) were reported for CdTe films deposited at low work pressures (2 and 5 mTorr), probably due to the tails in the band edges associated with defects in the lattice. Films deposited at higher pressures (from 8 to 40 mTorr) results with higher bandgap energies values than the reported for the bulk, which is attributed to the grain size reduction. From our results, better experimental conditions for CdTe films preparation were found at 35 W as rf-power and 5 mTorr as work pressure, given that higher energies tend to damage the films, to increase the mechanical stress and to reduce the crystallite size.

Acknowledgements: Authors thanks to J.E Corona, Dora Huerta, and Daniel Aguilar for their technical help. E. Camacho-Espinosa thanks Conacyt (México) and PIFI program by the support given during his academic interchange at Cinvestav Unidad-Mérida.

REFERENCE

- [1] D. L. Dreifus, R. M. Kolbas, R. L. Harper, J. R. Tassitino, S. Hwang, J. F. Schetzina, *Applied Physics Letters*.53 (1988) 1281. | [2] B. Yu, C. Zhu, F. Gan, *Journal of Applied Physics*.87(2000) 1761. | [3] J. Britt and C. Ferekides, *Applied Physics Letters*.62 (1993) 2852. | [4] C. S. Ferekides, U. Balasubramanian, R. Mamazza, V. Viswanathan, H. Zhao, D. L. Morel, *Solar Energy*. 77(2004) 830. | [5] S. J. Ikhmayies, R. N. Ahmad-Bitar, *Materials Science in Semiconductors Processing*.16(2013) 125. | [6] E. R. Shaaban, N. Afify, A. J. El-Taher, *Journal of Alloys and Compounds*.482 (2009) 404. | [7] N. A. Shah, A. Ali, A. Maqsood, *Journal of Non-Crystalline Solids*.355 (2009) 1478. | [8] A. Arnoult, J. Cibert, *Applied Physics Letters*.66 (1995) 2399. | [9] F. Golgovi, T. Visan, *Chalcogenide Letters*. 9(2012) 174. | [10] P. Bhattacharya, D. N. Bose, *Semiconductor Science and Technology*.6 (1991) 387. | [11] S. K. Pandey, U. Tiwari, R. Raman, C. Prakash, V. Krishna, V. Dutta, K. Zimik, *Thin Solid Films*. 473(2005)57. | [12] W. E. Hoke, R. Traczewski, *Journal of Applied Physics*.54(1983) 5089. | [13] A. U. Ubale, D. K. Kulkarni, *Indian Journal of Pure & Applied Physics*.44 (2006) 259. | [14] J. L. Boone, T. P. Van Doren, A. K. Berry, *Thin Solid Films*. 87(1982) 264. | [15] Y. O. Choi, N. H. Kim, J. S. Park, W. S. Lee, *Material Science and Engineering B*. 171(2010) 78. | [16] P. C. Sarmah, A. Rahman, *Bulletin of Materials Science*.21(1998) 154. | [17] A. D. Compaan, A. Gupta, S. Lee, S. Wang, J. Drayton, *Solar Energy*. 77(2004)822. | [18] K. Durose, D. Boyle, A. Abken, C. J. Ottley, P. Nolle, S. Degrave, M. Burgelman, R. Wendt, J. Beier, D. Bonnet, *Physica Status Solidi* 229 (2002)1064. | [19] M. Aguilar, A. I. Oliva, R. Castro-Rodriguez, J. L. Peña, *Journal of Materials Science: Materials in Electronics*.8 (1997)107. | [20] D. Wang, T. Narusawa, T. Kawaharamura, M. Furuta, C. Li, *Journal of Vacuum Science & Technology B*. 29(2011) 051205. | [21] S. Krishna, *Handbook of thin-film deposition processes and techniques*, second ed., Noyes Publications, United States, 2002. | [22] S. Kundu, S. Hazra, S. Banerjee, M. K. Sanyal, S. K. Mandal, S. Chaudhuri, A. K. Pal, *Journal of Physics D: Applied Physics*.31(1998) L77. | [23] H. R. Moutinho, F. S. Hasoon, F. Abulfotuh, L. L. Kazmerski, *Journal of Vacuum Science & Technology A*. 13(1995) 2883. | [24] S. Smith, R. Dhere, T. Gessert, P. Stradins, T. Wang, A. Mascarenhas, DOE Solar Energy Technologies Conference paper NREL/CP-590-37037, Denver Colorado, 2004, 1-2. | [25] L. Yan, J. A. Woollam, *Journal of Applied Physics*.92 (2002) 4392. | [26] Ch. Huimin, G. Fuqiang, Z. Baohua, *Journal of Semiconductors*.30 (2009) 053001. | [27] A. L. Patterson, *Physical Review*. 56(1939) 982. | [28] T. Markvart, L. Castañer, *Practical handbook of photovoltaics fundamentals and applications*, Elsevier, United Kingdom, 2003. | [29] R. D. Doherty, D. A. Hughes, F. J. Humphreys, J. J. Jonas, J. D. Jensen, M. E. Kassner, W. E. King, T. R. McNelly, H. J. McQueen, A. D. Rollet, *Material Science and Engineering*.A238 (1997)274. | [30] Vipin Chawla, R. Jayaganthan, Ramesh Chandra, *Journal of Materials Science & Technology*.26(2010) 678. | [31] A. M. Stoneham, *Journal of Physics C: Solid State Physics*. 10 (1977) 1179. | [32] E. Deligoz, K. Colakoglu, Y. Ciftci, *Physica B*. 373 (2006)130. | [33] K. Y. Chan, B. S. Teo, *Microelectronics Journal*. 38(2007)62. | [34] S. R. Reddy, S. A. Reddy, B. Radhakrishna, S. Uthanna, *Crystal Research & Technology*.47 (2012) 1104. | [35] W. L. Ting, Z. L. Tang, T. T. Ting, Y. Feng, *Chinese Physics Letters*.27 (2010) 027703. | [36] R. B. Kumar, S. T. Rao, *Digest Journal of Nanomaterials and Biostructures*, 7(2012)1061. | [37] J. Tauc, A. Abraham, R. Zallen, M. Slade, *Journal of Non-Crystalline Solids*. 4(1970) 279-288. | [38] J. Camassel, D. Auvèrgne, H. Mathieu, R. Triboulet, Y. Marfaing, *Solid State Communications*. 13(1973)68. | [39] Z. R. Khan, M. Zulfeqar, M. Sh. Khan, *Bulletin of Materials Science*.35 (2012)174. | [40] J. Musil, *Surface and Coating Technology*.125 (2000) 330. |